文章编号:1001-9014(2011)03-0198-04

Fabrication and characterization of $Cu(In,Ga)Se_2$ thin films

CUI Yan-Feng[1], YUAN Sheng-Zhao[1], WANG Shan-Li[2], HU Gu-Jin[1,2], CHU Jun-Hao[1,2]

(1. National Laboratory for Infrared Physics, Shanghai Institute of Technical Physics, Chinese Academy of Sciences, Shanghai 200083, China;
2. Shanghai Center for Photovoltaics, Shanghai 201201, China)

Abstract: $CuIn_{1-x}Ga_xSe_2$ (CIGS) is a promising direct band-gap semiconductor material for developing a new generation of high-efficiency and low-cost thin film solar cells due to its variable band-gap structure and high absorption coefficient in visible range. In this paper, a series of CIGS thin films were fabricated by combination of DC sputtering and selenizing processes. The effects of the sputtering power for deposition of $CuIn_{1-x}Ga_x$ (CIG) metal precursors and substrates on the microstructures and optical properties of the CIGS films were investigated. It was found that the film, deposited at 50W sputtering power onto Mo-coated soda lime glass (SLG) substrate and then selenized at 550℃ for 40minutes, exhibited a single chalcopyrite phase, uniform and dense morphology, and columnar grains. It is also found that the optical band gaps of the films are in the range of 1.21 ~ 1.24eV.

Key words: thin film solar cell; $CuIn_{1-x}Ga_xSe_2$ thin film; DC sputtering; selenizing
PACS: 68.55.-a, 73.61.Le, 84.60.Jt

$Cu(In,Ga)Se_2$ 薄膜的制备及其表征

崔艳峰[1], 袁声召[1], 王善力[2], 胡古今[1,2], 褚君浩[1,2]

(1. 中国科学院上海技术物理研究所 红外物理国家重点实验室, 上海 200083;
2. 上海太阳能电池研究与发展中心, 上海 201201)

摘要: $CuIn_{1-x}Ga_xSe_2$ (CIGS)为直接带隙半导体,其带隙宽度随In/Ga比而变化,且对可见光具有很高的吸收系数,是最有希望用于制作新一代高效、低成本薄膜太阳能电池的材料. 采用直流溅射和后硒化工艺制备了系列CIGS薄膜,研究了溅射功率和衬底对CIGS薄膜的微结构和光学性质的影响. 发现钼玻璃上溅射功率为50W,在550℃硒化40min的条件下获得的CIGS薄膜具有单一的黄铜矿结构、均匀致密的表面形貌和柱状晶粒. 所制备的薄膜的禁带宽度位于1.21 ~ 1.24 eV的范围.

关 键 词: 薄膜电池; $CuIn_{1-x}Ga_xSe_2$ 薄膜; 直流溅射; 硒化
中图分类号: TM914.4 **文献标识码**: A

Introduction

As one of the most promising semiconductor materials for developing high-efficiency, low-cost thin film solar cells, quaternary chalcopyrite compound $CuIn_{1-x}Ga_xSe_2$ (CIGS) has received extensive attention due to its tunable band-gap (1.0 ~ 1.7eV), high absorption coefficient (over $10^5 cm^{-1}$), and high stability. So far, power conversion efficiency as high as 19.9% has been achieved for CIGS thin film solar cells in laboratory[1]. A variety of methods have been used to prepare CIGS thin films for optical absorption layer, including

Received date: 2010-05-31, **revised date**: 2010-07-05 **收稿日期**: 2010-05-31, **修回日期**: 2010-07-05
Foudantion item: Supported by National Basic Research Program of China (973 program, Grant No. 2010CB933700), National Natural Science Foundation of China (Grant No. 10774154), Knowledge Innovation Program of the Chinese Academy of Sciences, and Shanghai City Committee of Science and Technology in China (Grants No. 08JC1420900 and 0452nm085)
Biography: CUI Yan-Feng(1982-), female, Qindao, Shandong, PhD. candidate. Research area involves the fabrication and characterization of novel photovoltaic materials and devices. E-mail: cuiyanfeng_0517@yahoo.com.cn.

co-evaporation[2], magnetron sputtering[3], pulsed laser deposition[4], electro-deposition[5], selenization of metallic precursors[6], and so on. Among these methods, selenization of metallic precursors is the best choice for large scale applications. However, this approach requires highly toxic H_2Se gas generally, making it undesirable.

In the present work, a two-step process was used to prepare CIGS thin films. The metallic precursor $CuIn_{1-x}Ga_x$ (CIG) was first deposited on substrates by a DC sputtering method, and then was selenized under Se vapor instead of toxic H_2Se gas. The dependence of the microstructures, morphologies, and optical properties of the CIGS films on the sputtering power of CIG metal precursors was explored. To the best of our knowledge, there are few reports on the influence of sputtering powers of precursors and substrates on the CIGS films.

1 Experiment

All the films for this study were deposited on Mo-coated soda lime glass, SLG and SiO_2 substrates. The Mo-back-contact was fabricated by DC sputtering and the thickness was about 1μm. CIGS films were prepared by a two-step process. Firstly, the metallic precursors were deposited by DC sputtering using a ternary $Cu_{32.37}In_{54.6}Ga_{13.03}$ (≥99.9wt%) target at room temperature. The background pressure of the sputtering was 5×10^{-6} mbar and the working gas was high purity (>99.9%) of Ar gas. During the deposition process, the working pressure and the deposition time were fixed to be 1Pa and 10 minutes, respectively. The stoichiometric ratio of metallic precursors was adjusted by changing the sputtering power. Secondly, the as-deposited metallic precursors were selenized in a quartz tube furnace with a vacuum level of 10 mtorr, and the precursor samples were put in a graphite box. The selenization process was carried out in two stages. In the first stage, the metallic precursor was treated at 250℃ for 30min to assure the sufficient reaction between the precursors and the Se. In the second stage, the specimens were heated to 550℃ and kept for 40min to ensure that the metallic precursor has been fully converted into the CIGS.

The crystal structures of the films were determined by X-ray diffraction (XRD) using BrukerD8 diffractometer with CuK_α radiation. The surface morphology was measured by a PhilipsS360 scanning electron microscope (SEM). The optical properties were characterized by a Perklin Elmer-Lambda 2s in the wavelength range of 300 ~ 1100 nm. The thicknesses of the samples were obtained using a DEKTAK profilometer.

2 Results and discussion

Figure 1 shows the XRD patterns for the CIGS films fabricated at 50 W, 60W, and 70W sputtering powers, respectively. The inset is an enlarged view for those peaks marked by (312/116). As shown in Fig. 1, the peaks locating at $2\theta = 40.50°$ and 73.68° belong to the Mo phase, and the three sharply main peaks, locating at $2\theta = 26.69°$, 44.29° and 52.51°, correspond to (112), (220/204) and (312/116) orientation of $CuIn_{0.7}Ga_{0.3}Se_2$, respectively. The experimental results indicate that all the CIGS films have a single chalcopyrite phase. From the inset in Fig. 1, it can be seen that the positions of the main Braggs peaks of films shift slightly to the larger angles with increasing sputtering power, similar to those reported in literatures[7,8]. M. Venkatachalam et al. suggested that the peaks shift to the higher diffraction angle is due to an increase of gallium concentration in film[9]. So we deduce that the gallium content decreases with decreasing the sputtering power. The atomic radius of Ga is less than In atom. Smaller Ga atoms substituting indium in the cell causes a shrinkage of the lattice, which decreases the lattice constant d and results in a larger value of 2θ. From the analysis of the EDS composition of the films which shown in Table 1, we can see that the gallium concentration increases with the increase of the sputtering power, which is in agreement with the result of XRD. All samples are nearly stoichiometric and slightly Cu-deficient, which may be suitable as optical absorber for a solar cell[10].

Table 1　Composition of the prepared CIGS thin films by EDS

表 1　EDS 测得的 CIGS 薄膜的组分

Sample	Cu (at %)	In (at %)	Ga (at %)	Se (at %)	Cu/(In+Ga)	Ga/(In+Ga)
60W	23.41	19.22	7.78	49.59	0.87	0.29
50W	23.02	18.14	6.98	51.86	0.92	0.28
70W	24.95	20.79	9.38	44.88	0.83	0.31

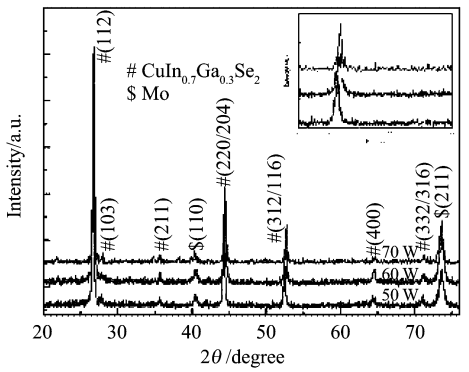

Fig. 1 XRD patterns for the CIGS films fabricated at different sputtering power

图1 不同溅射功率制备的 CIGS 薄膜的 XRD 图

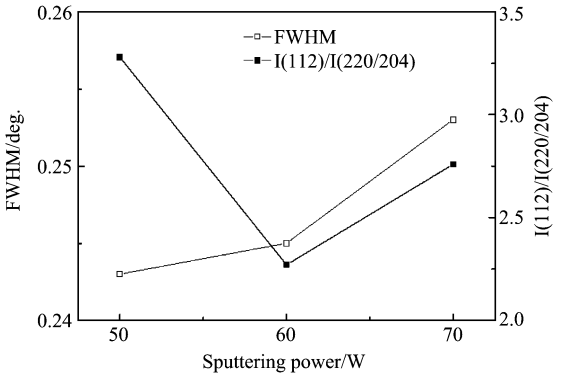

Fig. 2 FWHM of (112) diffraction peaks and peak intensity ratios of the (112)/(220/204) planes for CIGS films fabricated at different sputtering power

图2 不同溅射功率制备的 CIGS 薄膜的(112)晶向的半高宽和(112)/(220/204)强度比

The full width of half maximum (FWHM) values of (112) diffraction peaks and the peak intensity ratios of the (112)/(220/204) planes for CIGS films fabricated at different sputtering power are depicted in Fig. 2. As we can see that the FWHM values increase with the increase of the sputtering power. Based on Scherrer's formula the average crystallite size decreases with increasing the power, and the sample of 50W may have the biggest grain size. Also from the result of peak intensity ratio of the (112)/(220/204) planes we can see the preferred (112) orientation in the sample of 50W is the strongest, which indicates better crystallinity.

The XRD diagrams and FWHM of (112) diffraction peaks and peak intensity ratios of the (112)/(220/204) planes for CIGS films deposited onto different substrates are presented in Fig. 3 and Fig. 4. The substrater of sample1, 2 and 3 are SLG/Mo, SLG and

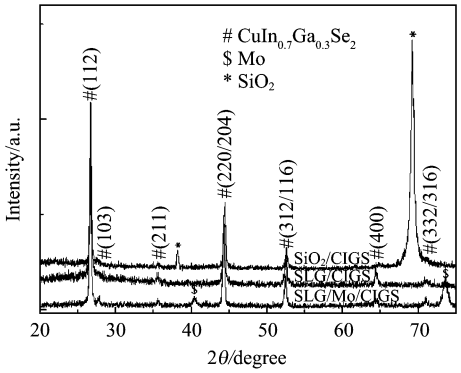

Fig. 3 XRD diagrams for the CIGS films deposited onto different substrates

图3 不同衬底上沉积的 CIGS 薄膜的 XRD 图

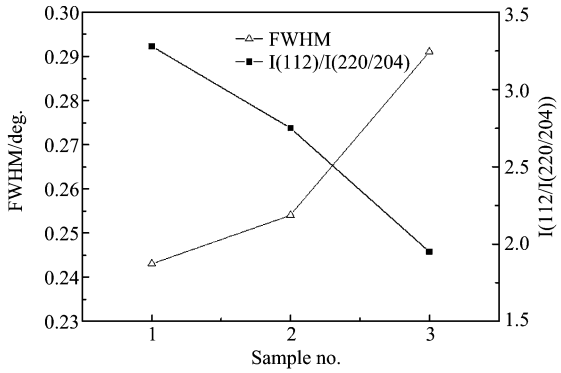

Fig. 4 FWHM of (112) diffraction peaks and peak intensity ratios of the (112)/(220/204) planes for CIGS films fabricated on different substrates

图4 不同衬底上沉积的 CIGS 薄膜(112)晶向的半高宽和(112)/(220/204)强度比

SiO_2 as shown in Fig. 3, all films have three sharply main peaks corresponding to (112), (220/204) and (312/116) orientation of $CuIn_{0.7}Ga_{0.3}Se_2$, which indicates that all the CIGS films have a single chalcopyrite phase and no other phases. The film grown onto the SLG/Mo substrate presents stronger intensity in (103) and (332/316) planes comparing with films grown onto SLG and SiO_2 substrates, indicating higher crystallinity. Also from the analysis of FWHM of (112) diffraction peaks and peak intensity ratios of the (112)/(220/204) planes shown in Fig. 4, we conclude that the CIGS films deposited onto the Mo/SLG substrates have bigger grain size and higher crystallinity than films deposited onto SLG and SiO_2 substrates.

The surface SEM micrographs for CIGS thin films fabricated at various sputtering power and different substrates are shown in Fig. 5. As displayed in Fig. 5, the

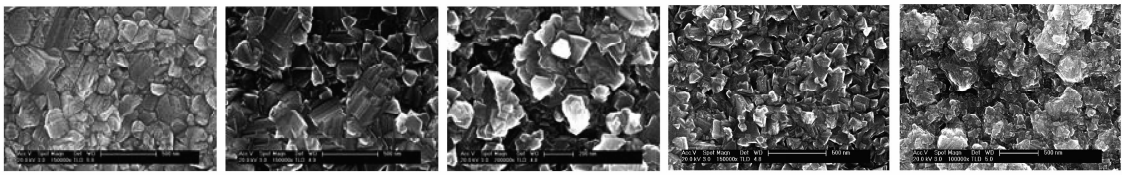

Fig. 5　SEM micrographs for CIGS films (a)50W, SLG/Mo/CIGS (b)60W, SLG/Mo/CIGS (c)70W, SLG/Mo/CIGS (d)60W, SLG/ CIGS (e)60W, SiO_2/CIGS

图 5　CIGS 薄膜的表面 SEM 图 (a)50W, SLG/Mo/CIGS (b)60W, SLG/Mo/CIGS (c)70W, SLG/Mo/CIGS (d)60W, SLG/ CIGS (e)60W, SiO_2/CIGS

CIGS film sputtered at 50W onto the SLG/Mo substrate has a relative uniform and dense morphology, and the grain shape is more regular and the distribution of grain sizes is narrower in film, whereas, the CIGS film at 60W or 70W onto the SLG/Mo substrates possesses some of pinholes and microcracks in the surface of the film. The films grown onto the SLG and SiO_2 substrates have smaller grains and no regular grains. To achieve a high power conversion efficiency, it is desirable that the absorber layer not only is dense but also has large size and columnar grains in a polycrystalline thin film solar cell. The columnar microstructure facilitates the current transport and reduces the recombination of the photon-generated carriers, and the dense bulk film is beneficial to suppress dark current in a solar cell.

Since the morphology of the $CuIn_{1-x}Ga_xSe_2$ thin film is dependent on the CIG alloy precursor, a smooth surface of precursor is essential to fabricate a high-quality solar cell [3]. With the increasing of sputtering power of CIG precursors, the atomic kinetic energy and the migration increase, giving rise to the formation of a rough surface precursor films, and further to the formation of pinholes and microcracks after the selenization treatment for samples (b) and (c). The influence of substrates on the films may be attributed to the incorporation of Na and the $MoSe_2$ interfacial layer formed at the interface CIGS/Mo[11].

Figure 6 presents the optical absorbance (A) spectra of three investigated CIGS films. The thicknesses of the films are estimated to be within the range of 1 ~ 1.6μm. We can evaluate the band gap energy E_g from Fig. 6 according to the method described by Shankar et al. by extrapolating the tangent line of the *A-E* curves to the x-axis[12]. The calculated band gaps

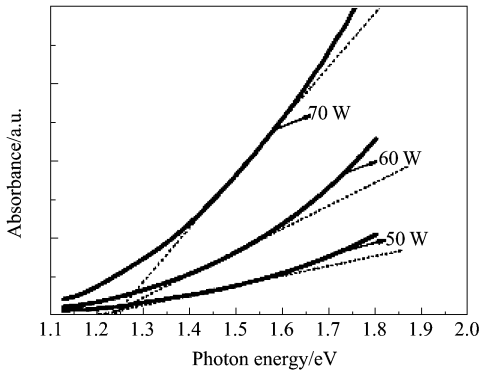

Fig. 6　Absorbance versus photon energy for CIGS films sputtered at various powers

图 6　不同溅射功率制备的 CIGS 薄膜的 *A-E* 图

for samples (a), (b), and (c) are 1.21, 1.23 and 1.24 eV, respectively, which are well in accordance with results reported by other researchers[13]. It should be noted that in the calculation of E_g the optical loss form, the reflection and the scattering aroused by rough surface and grains were not considered, and the obtained E_g is an estimated value.

The band gap E_g of CIGS films changes with the variation of Ga/(In + Ga) ratio, x, in the form of

$$E_g(\text{eV}) = 1.02 + 0.67x + bx(x-1) \quad , (1)$$

where b is the optical bowing coefficient between 0.11 and 0.24[14]. Wei and Zhang et al.[15] have observed that with reducing x , the valence band maximum of CIGS increases slightly and the conduction band minimum decreases significantly. Thus, we suggest that the addition of Ga affects the lattice parameters and crystal structure. The difference between the electronegativity of In^{3+} and Ga^{3+} ions causes the change of the band gap when In in the CIS film is substituted partially by Ga[13].

(下转 206 页)

3679—3682.
[9] NAYAK B, EATON B, SELVAN J, *et al*. Semiconductor laser crystallization of a-Si: H on conducting tin-oxide-coated glass for solar cell and display application[J]. *Applied Physics A*, 2005, **80**(5): 1077—1080.
[10] ZHANG Shi-Bin, LIAO Xian-Bo, AN Long, *et al*. Micro-Raman study on hydrogenated protocrystalline silicon films [J]. *Acta Physica Sinica*, (张世斌, 廖显伯, 安龙, 等. 非晶/微晶过渡区域硅薄膜的微区喇曼散射研究. **物理学报**), 2002, **51**(8): 1811—1815.
[11] VOUTSAS A, HATALIS M, BOYCE J, *et al*. Raman spectroscopy of amorphous and microcrystalline silicon films deposited by low-pressure chemical vapor deposition [J]. *Journal of Applied Physics*, 1995, **78**(12): 6999—7006.
[12] MURAKAMI K, ERYU O, TAKITA K, *et al*. Explosive crystallization starting from an amorphous-silicon surface region during long-pulse laser irradiation[J]. *Physical Review Letters*, 1987, **59**(19): 2203—2206.

(上接201页)

3 Conclusion

CIGS thin films have been successfully prepared by a two-step process with solid Se powder instead of toxic H_2Se gas onto Mo-coated soda lime glass, SLG and SiO_2 substrates. It has been found that the sputtering power and substrates have a significant effect on the microstructure, surface morphology, composition, and optical performance of CIGS films. The XRD and EDS data indicate that each film has a single chalcopyrite structure, and the gallium concentration in the film increases with the increased sputtering power of precursors. The SEM pictures show that the film sputtered at 50W onto the SLG/Mo substrate exhibits a more uniform and dense surface and larger size columnar grains. The band gaps for samples obtained at the sputtering power of 50W, 60W and 70W were estimated to be 1.21, 1.23 and 1.24 eV, respectively. The fabricated CIGS films may be suitable for the application in the environmental friendly thin film solar cell.

Acknowledgements

The authors thank Prof. Zh. M. Huang, P. P. Chen, Drs. F. W. Shi, J. H. Ma, Y. F Liu, and Y. H. Zhan for their help in the experimental measurements and valuable discussions on experimental data.

REFERENCES

[1] Repins I, Contreras M A, Egaas B, *et al*. 19.9%-efficient ZnO/CdS/$CuInGaSe_2$ Solar Cell with 81.2% Fill Factor [J]. *Prog. Photovolt: Res. Appl.*, 2008, **16**: 235—239.
[2] Negami T, Hashimoto Y, Nishiwaki S. Cu(In, Ga)Se_2 thin-film solar cells with an efficiency of 18% [J]. *Solar Energy Materials & Solar Cells*, 2001, **67**: 331—335.
[3] Song Ho-Keun, Kim Soo-Gil, Kim Hyeong-Joon, *et al*. Preparation of $CuIn_{1-x}Ga_xSe_2$ Thin Films by Sputtering and Selenization Process [J]. *Solar Energy Materials and Solar cells*, 2003, **75**: 145—153.
[4] Negami T, Satoh T, Hashimoto Y, *et al*. Large-area CIGS Absorbers Prepared by Physical Vapor Deposition[J]. *Solar Energy Materials and Solar Cells*, 2001, **67**: 1—9.
[5] Fernfindez A M, Bhattacharya R N. Electrodeposition of $CuIn_{1-x}Ga_xSe_2$ Precursor Films: optimization of Film Composition and Morphology [J]. *Thin Solid Films*, 2005, **474**: 10—13.
[6] Liu Wei, Tian Jian-Guo, He Qing, *et al*. The influence of alloy phases in the precursors on the selenization reaction mechanisms [J]. *J. Phys. D: Appl. Phys.*, 2009, **42**: 1—5.
[7] Moussa G W El Haj, Ajaka M, Tahchi M. El, *et al*. Ellipsometric spectroscopy on polycrystalline $CuIn_{1-x}Ga_xSe_2$: Identification of optical transitions [J]. *Phys. Stat. Sol.* (*a*), 2005, **202**: 469—475.
[8] Dejene F B, Alberts V. Structural and optical properties of homogeneous Cu(In, Ga)Se_2 thin films prepared by thermal reaction of InSe/Cu/GaSe alloys with elemental Se vapour [J]. *J. Phys. D: Appl. Phys.*, 2005, **38**: 22—25.
[9] Venkatachalam M, Kannan M D, Jayakumar S, *et al*. Effect of annealing on the structural properties of electron beam deposited CIGS thin films [J]. *Thin Solid Films*, 2008, **516**: 6848—6852.
[10] Rockett A. The Electronic effects of point defects in $CuIn_{1-x}Ga_xSe_2$ [J]. *Thin Solid Films*, 2000, **361—362**: 330—337.
[11] Assmann L, Berne`de J C, Drici A, *et al*. Study of the Mo thin films and Mo/CIGS interface properties[J]. *Applied Surface Science*, 2005, **246**: 159—166.
[12] Shankar K, Tep K C, Mor G K, *et al*. An electrochemical strategy to incorporate nitrogen in nanostructured TiO_2 thin films: modification of bandgap and photoelectrochemical properties[J]. *J. Phys. D: Appl. Phys.*, 2006, **39**: 2361—2366.
[13] Bouabid K, Ihlal A, Manar A, *et al*. Effect of deposition and annealing parameters on the properties of electrodeposited $CuIn_{1-x}Ga_xSe_2$ thin films[J]. *Thin Solid Films*, 2005, **488**: 62—67.
[14] Lundberg O, Edoff M, Stolt L. The effect of Ga-grading in CIGS thin film solar cells[J]. *Thin Solid Films*, 2005, **480—481**: 520—525.
[15] Wei Su-Hai, Zhang S B, Zunger A. Effects of Ga addition to $CuInSe_2$ on its electronic, structural, and defect properties[J]. *Appl. Phys. Lett.*, 1998, **72**: 3199—3201.